Title: Inactivation of thermogenic UCP1 as a historical contingency in multiple placental mammal clades

Authors: Michael J. Gaudry[1], Martin Jastroch[2], Jason R. Treberg[1,3], Michael Hofreiter[4]†, Johanna L.A. Paijmans[4†], James Starrett[5‡], Nathan Wales[6], Anthony V. Signore[1§], Mark S. Springer[5] and Kevin L. Campbell[1*]

Affiliations:

[1]Department of Biological Sciences, University of Manitoba, Winnipeg, MB, R3T 2N2, Canada.

[2]Institute for Diabetes and Obesity, Helmholtz Zentrum München, German Research Center for Environmental Health, Parkring 13, 85748 Garching, Germany.

[3]Department of Human Nutritional Sciences, University of Manitoba, Winnipeg, MB, R3T 2N2, Canada.

[4]Department of Biology, The University of York, Heslington, York, YO10 5DD, UK.

[5]Department of Biology, University of California, Riverside, CA 92521, USA.

[6]Centre for GeoGenetics, Natural History Museum of Denmark, Øster Voldgade 5-7, 1350 Copenhagen, Denmark.

[†]Current address: Universität Potsdam, 14476 Potsdam, Germany.

[‡]Current address: San Diego State University, San Diego, California 92182, USA.

[§]Current address: University of Nebraska, Lincoln, Nebraska 68588, USA.

*Correspondence: Kevin.Campbell@umanitoba.ca

Abstract: Mitochondrial uncoupling protein 1 (UCP1) is essential for non-shivering thermogenesis in brown adipose tissue and is widely accepted to have played a key thermoregulatory role in small-bodied and neonatal placental mammals that enabled the exploitation of cold environments. Here we map *ucp1* sequences from 133 mammals onto a 51-kb species tree and show that inactivating mutations have occurred in at least eight of the 18 traditional placental orders, thereby challenging the physiological importance of UCP1 across Placentalia. Selection and timetree analyses further reveal that *ucp1* inactivations temporally correspond with secondary reductions in metabolic intensity in xenarthrans and pangolins, or coincided with a ~30 million year episode of global cooling in the Paleogene that promoted sharp increases in body mass and cladogenesis evident in the fossil record of other lineages lacking a functional UCP1. Our findings also demonstrate that members of various lineages (*e.g.*, cetaceans, horses, woolly mammoths, Steller's sea cows) evolved extreme cold hardiness in the absence of UCP1-mediated thermogenesis. Finally, we identify *ucp1* inactivation as a historical contingency that is linked to the current low species diversity of UCP1-less clades, thus providing the first evidence of species selection related to the presence or absence of a single gene product.

Main Text: Adaptive non-shivering thermogenesis (NST) of placental mammals is predominantly mediated by uncoupling protein 1 (UCP1), which resides at high levels in the mitochondrial inner membrane of brown adipose tissue (BAT) (*1*). Upon activation, UCP1 facilitates proton leak into the mitochondrial matrix (*2*) without concomitant ATP production, thereby intensifying substrate oxidation and hence cellular heat production. BAT deposits are located adjacent to major blood vessels in the neck, thorax, and

abdomen to promote the rapid distribution of NST heat (*3*). In addition to its strategic location, the observation that chronic cold stress stimulates the proliferation and activity of BAT (*4*), highlights the canonical importance of NST for small-bodied and torpor expressing placental mammals, together with neonates of larger cold-tolerant species (*5*). UCP1 has also been implicated in the regulation of food intake, energy balance, the fever response, the prevention of cold-induced oxidative stress, and possibly even longevity (*6-9*). The recent discovery of UCP1 induction in a class of white adipocytes (termed brite or beige fat) in response to exercise and cold exposure moreover offers therapeutic interventions for obesity, hyperlipidemia, cachexia, and other metabolic disorders (*10, 11*).

The presence of non-thermogenic UCP1 in marsupials, monotremes, as well as both ray-finned and lobe-finned fishes (*12*) indicates that *ucp1* was likely recruited for NST sometime during the Mesozoic ancestry of placental mammals (*13, 14*). This ancestor is reconstructed as a small (6 to 245 g) nocturnal insectivore that gave birth to hairless, altricial young and likely exhibited torpor (*i.e.*, heterothermy) (*15, 16*). Facultative BAT thermogenesis may have evolved to defend against the natural cold stress of birth (*17*), to decrease the energetic costs of rewarming from torpor (*18*), or to enable endothermy during the reproductive season (*19*), and is postulated to underlie the subsequent radiation of crown eutherians into cold environments (*3*). Evolution of this thermogenic tissue was presumably also driven by small body size as maximal NST capacity is inversely proportional to mass, with little to no thermal contribution predicted in mammals above 10 kg (*20*). Although limited data are available for larger bodied species, *ucp1* is only transiently expressed in BAT deposits of neonatal cattle (~40 kg; *21*) and pre-weaned

harp seals (<30 kg; *22*), with minor depots either absent or present in adult humans (*11*). Conversely, the persistence of UCP1 in BAT depots of subadult harbor seals (34–38 kg; *5*) and the discovery of a large cervical mass of fat that is histologically similar to BAT in a preserved 1-month old (~100 kg) woolly mammoth (*23*), but not extant elephants, implies this tissue may underpin the evolution of extreme cold hardiness in at least some larger-bodied species. Consistent with this hypothesis, *ucp1* inactivation is only documented within the pig lineage whose newborn lack discernible BAT and are notoriously cold intolerant (*17, 24*).

Support for a *de novo* gain of thermogenic function in early eutherians is bolstered by an elevated rate of nucleotide substitutions on the stem placental branch (*13, 14*), though these results were based on limited sample sizes (10 and 16 species, respectively) and heavily biased towards small-bodied forms from only two (Euarchontoglires and Laurasiatheria) of the four major clades of placental mammals. As body size and energetic considerations are expected to alter the selective advantage of BAT-mediated NST, we hypothesized that evolution of large body size or reduced thermogenic capacity would be accompanied by relaxed selection on the *ucp1* locus.

Our phylogenetically informed analysis (*25*) of 141 vertebrate species (table S1) support this contention and reveal independent inactivating mutations of *ucp1* (including exon deletions) in the ancestors of at least eight placental clades: xenarthrans (Cingulata and Pilosa), pangolins (Pholidota), dolphins and whales (Cetacea), sea cows (Sirenia), elephants (Proboscidea), hyraxes (Hyracoidea), pigs (Suidae), and horses, donkeys, and zebras (Equidae) (Figs. 1, 2 and fig. S1). Notably, these findings are corroborated by a signature of neutral evolution (ω=0.94 in pseudogenic branches vs. 0.16 in species

containing an intact *ucp1* locus; table S2 and data file S1) and a lack of discernable BAT in neonates of each of these groups (*17*). To better facilitate comparisons between the genomic record and fossil record, and identify potential climatic and ecological factors underlying *ucp1* loss in these lineages, we calculated gene inactivation date ranges based on a 51-kb molecular timetree (data file S2) and d*N*/d*S* ratios (*25*) in functional, pseudogenic, and mixed branches (where *ucp1* inactivation was deemed to have occurred; *26*).

The earliest disruptions of *ucp1* function (likely Cretaceous; Fig. 3 and table S3) occur in the ancestors of xenarthrans and pangolins, two groups that exhibit remarkable convergence in many ecological, morphological, and physiological traits and which are generally characterized by 'inferior' temperature-regulating mechanisms, and low, labile body temperatures (*27-30*). The ancient inactivations of *ucp1* in these lineages may in part underlie this convergence and are presumably linked to secondary reductions in metabolic intensity associated with the energy poor diets and ancestral burrowing habits of these taxa (*28, 29*). While BAT-mediated NST has been shown to enhance cold tolerance (*31*) and accelerate rewarming from torpor at a reduced net energy cost (*18*), at least some xenarthrans exhibit torpor (*30*) while others exploited thermally taxing environments. The latter was presumably enabled by elaborate countercurrent heat exchangers (arteriovenus rete) in the limbs that promote heat conservation (*32*) which, coupled with a relatively thick pelt and the recurrent development of gigantism (*33*), likely facilitated the colonization of subarctic environments (68ºN) by the Pleistocene sloth *Megalonyx jeffersonii* (*34*) and the aquatic niche by Miocene/Pliocene marine sloths of the genus *Thalassocnus* (*35*).

For the remaining six lineages, our estimates suggest *ucp1* was predominantly silenced from the early Eocene to the late Oligocene, a period characterized by marked global cooling (Fig. 3) that spurred the diversification of grass and deciduous woodland communities (*36*). As these factors have been proposed to underlie body mass increases of numerous mammalian groups during the Cenozoic (*37*), we assembled a dataset (*25*) to explore potential links between mammalian body size evolution and *ucp1* inactivation (table S3). In each case, our *ucp1* inactivation date ranges overlap or immediately precede magnitude scale increases in body size (Fig. 4A). For example, the earliest proboscideans (59-60 million year old [Ma] *Eritherium*; *38*) and hyraxes (~55 Ma *Seggeurius*; *39*) were small (~3-5 kg), but gave rise to much larger species (*e.g.*, 3600 kg *Barytherium* and 800–1400 kg *Titanohyrax ulitimus*) coincident with our estimates of *ucp1* inactivation. Although large-bodied (~625–800 kg) hyracoids, *e.g.*, '*Titanohyrax*' *mongereaui*, are also known from earlier deposits, the presence of only a single, 'primitive' *Seggeurius*-sized species (*Dimaitherium patnaiki*) from the early Priabonian (~37 Ma), suggests that gigantism evolved independently in mid- and late-Eocene hyracoids (*40*). Our estimate of *ucp1* inactivation in the family Equidae (25.1–20.7 Ma) is also coincident with an ~8-10 fold increase in body size in this lineage (Fig. 4A). Potential thermogenic limitations arising from UCP1 loss (see *24*) were clearly no impediment to the equines' ability to exploit cold environments given "that Alaskan horses prospered during the LGM [last glacial maximum; ~18,000 years ago], and appear to have been particularly well adapted to the more intense versions of the cold/arid Mammoth Steppe" (*41*).

We estimate *ucp1* inactivation in Cetacea occurred soon after their divergence from hippopotamids (~52.75 Ma), and document the complete deletion of this locus in delphinids (Fig. 2B) by the late Miocene. These findings directly contradict recent claims of UCP1 expression in blubber of four delphinoid species (*42*) (which we attribute to unspecific antibody hybridization to UCP1 paralogs in this tissue), and intact UCP1 proteins in the genomes of six cetacean species (including bottlenose dolphin and killer whale; *43*). Notably, the non-delphinid cetacean UCP1 sequences in the latter study exhibit premature stop codons stemming from both nonsense and frameshift mutations (as also seen in Fig. 1), while the killer whale and bottlenose dolphin 'UCP1' sequences correspond to UCP2 and UCP3, respectively. Consequently, the pseudogenization of *ucp1* immediately predates strong increases in body size during the early amphibious stages of archaeocete evolution (*i.e.*, from 15–30 kg *Himalayacetus* [52.5 Ma] to 590–720 kg *Ambulocetus*/*Rodhocetus* [48 Ma]; *44-45*), with similar scale body mass changes following the inactivation of *ucp1* in sirenians 46.0-44.8 Ma (Fig. 4A). It is notable that loss of UCP1 function does not appear to be linked to the advent of aquatic birth in these lineages (pinnipeds and other semi-aquatic mammals are born on land or ice and generally do not enter the aquatic environment until after weaning) as our estimates of *ucp1* inactivation precede the loss of hindlimb land locomotion—and hence emergence of fully aquatic lifestyles—in primitive dugongids (*46*) and early basilosaurids (*e.g.*, *Basilosaurus*, *Durodon*; *47*) during the Bartonian by 5 to 10 Ma. Notably, absence of UCP1-mediated NST is not mechanistically linked with inferior thermoregulatory capabilities in neonates of either lineage as evidenced by year-round resident high-Arctic whales (*e.g.*, bowhead, beluga, and narwhal) and the recently extinct sub-Arctic Steller's

sea cow (*Hydrodamalis gigas*). The presence of a pseudogenic copy of *ucp1* in woolly mammoths further precludes a UCP1-mediated thermogenic function for the BAT-like tissue described from a 1-month old specimen (*23*), and again illustrates that *ucp1* is not uniquely associated with the evolution of extreme cold hardiness in placental mammals.

In light of the apparent link between *ucp1* inactivation and body mass (Fig. 4A), it is perhaps surprising that *ucp1* is intact and ostensibly evolving under purifying selection in large-bodied rhinoceros, pinnipeds (walrus, Weddell seals, harbor seals), and hippopotamuses (ω=0.25 to 0.29; table S2). However, relatively low ω values for these branches should be treated with caution in the absence of protein expression and functional data, as long branches may conflate multiple evolutionary histories (*i.e.*, a recent transition to neutral selection that is obscured by a much longer period of purifying selection). Conversely, the intact *ucp1* locus of camels intriguingly exhibits a signature of neutral evolution (ω=1.03; table S2) coupled with a four-residue deletion within a highly conserved region of the third matrix loop that borders the GDP-binding domain, which may compromise its function (fig. S2).

In addition to abrupt changes in body mass (Fig. 4A), the inactivation of *ucp1* also coincided with rapid species diversification evident in the fossil record of these lineages (Fig. 4B), consistent with recent work linking increased body mass with cladogenesis (*48*). Notably, however, as most lineages lacking a functional UCP1 currently exhibit relatively low species diversities, we performed analyses (*25*) with binary state speciation and extinction (BiSSE; *49*), as implemented in the diversitree package for R (*50*), to determine if diversification rates among extant placental mammals have been higher in taxa that retain a functional copy of this gene ('UCP1-plus') versus taxa that have a

pseudogenic copy of this gene ('UCP1-minus'). These analyses provide strong statistical support ($p \leq 0.000023$) that diversification rates have been higher in UCP1-plus taxa than UCP1-minus taxa (table S4).

Although NST is often thought to be an effective means to counter low ambient temperatures, heavy reliance on thermogenesis comes at a high energetic cost that may be difficult to meet in species that consume energy poor diets and exhibit reductions in metabolic intensity (xenarthrans and pangolins). Selection pressures favouring larger body size are also predicted to reduce reliance on BAT by decreasing the relative surface area for heat loss (*20*) and enabling the development of size-dependent heat conservation measures (*e.g.*, countercurrent rete). This selection may have been expected to favour precocial species due to their heightened insulation at birth and generally transient reliance on BAT-mediated NST relative to altricial taxa (*51*). In this context, it is notable that only one of the eight lineages lacking a functional *ucp1* locus is altricial (pangolins). The regressive evolution of *ucp1* together with attendant increases in body mass may thus have contributed to the initial exploitation of seasonal temperate niches (and other large-bodied terrestrial and aquatic habitats vacated by dinosaurs/marine reptiles following the KPg extinction) by these lineages and presumably underlies their rapid diversification apparent in the fossil record (Fig. 4B).

This evolutionary success was, however, not devoid of negative long-term fitness consequences. For example, the re-evolution of small body size (<5 kg) is presumably constrained by competitive disadvantages versus species with UCP1-mediated NST, or has restricted medium-sized members of these lineages to tropical/subtropical environments (*i.e.*, xenarthrans, pangolins, hyraxes). These factors coupled with

observations that large-bodied taxa exhibit higher risks of extinction (*52*) lead us to hypothesize that loss of UCP1-dependent thermogenesis may represent a historical contingency that underlies the current low species diversity of placental clades lacking a functional *ucp1* gene (Fig. 4B). This assertion is supported by our BiSSE analyses, as we demonstrate higher diversification rates in UCP1-plus taxa than UCP1-minus taxa. To our knowledge, these results provide the first evidence that links diversification rates and hence species selection to the presence or absence of a single gene product.

The observation that brown-throated sloths (*Bradypus variegatus*) exposed to cold exhibit markedly improved temperature regulation abilities when pregnant (*29*) suggests the presence of inducible NST mechanism(s) in this and potentially other clades lacking a functional UCP1. One candidate recently implicated in muscle-based NST is sarcolipin (*sln*; *53, 54*), which intriguingly exhibits two unique residue deletions in equids that may alter ATP-dependent Ca^{2+} uptake in skeletal muscle, though is disrupted in extant sloths (fig. S3). It is unlikely that other paralogs (*i.e.*, *ucp2* and *ucp3*) assumed a UCP1-like role in BAT and/or beige fat in these species as d*N*/d*S* analyses failed to identify differential selection acting upon these loci in branches where *ucp1* was lost (data files S3-S4). Importantly, these ancillary analyses pinpoint additional pseudogenization events (*e.g.*, *ucp2* and *ucp3* inactivation in armadillos [table S5]) that provide natural model systems to help elucidate the precise function of these proteins. As adult and obese humans possess only negligible brown adipose depots, species lacking UCP1 moreover provide unexplored model systems for adipocyte remodeling and alternative pathways of thermogenesis in response to cold that may be more transformative to biomedical applications. Taken together, our findings raise important questions regarding the roles

and physiological significance of uncoupling proteins over the course of eutherian evolution, challenge the perception that BAT underlies cold tolerance in large-bodied eutherian mammals, and identify *ucp1* inactivation as a historical contingency that may underlie the current low species diversity of these clades.

References and Notes:

1. D. G. Nicholls, R. M. Locke, *Physiol. Rev.* **64**, 1-64 (1984).
2. G. M. Heaton, R. J. Wagenvoord, A. Kemp, D. G. Nicholls, *Eur. J. Biochem.* **82**, 515-521 (1978).
3. B. Cannon, J. A. N. Nedergaard, *Physiol. Rev.* **84**, 277-359 (2004).
4. J. Rafael, P. Vsiansky, G. Heldmaier, *J. Comp. Physiol. B* **155**, 717-722 (1985).
5. Y. Sakurai *et al.*, *Mar. Mam. Sci.* **31**, 818-827 (2015).
6. B. Cannon, J. Houstek, J. A. N. Nedergaard, *Ann N. Y. Acad. Sci.* **856**, 171-187 (1998).
7. H. M. Feldmann, V. Golozoubova, B. Cannon, J. Nedergaard, *Cell Metab.* **9**, 203-209 (2009).
8. A. Stier *et al.*, *J. Exp. Biol.* **217**, 624-630 (2014).
9. V. Golozoubova *et al.*, *FASEB J.* **15**, 2048-2050 (2001).
10. M. Petruzzelli *et al.*, *Cell Metab.* **20**, 433-447 (2014).
11. E. D. Rosen, B. M. Spiegelman, *Cell* **156**, 20-44 (2014).
12. M. Jastroch, S. Wuertz, W. Kloas, M. Klingenspor, *Physiol. Genomics* **22**, 150-156 (2005).
13. S. Saito, C. T. Saito, R. Shingai, *Gene* **408**, 37-44 (2008).
14. D. A. Hughes, M. Jastroch, M. Stoneking, M. Klingenspor, *BMC Evol. Biol.* **9**, 4 (2009). doi:10.1186/1471-2148-9-4.
15. M. A. O'Leary *et al.*, *Science* **339**, 662-667 (2013).
16. B. G. Lovegrove, *Biol. Rev. Camb. Philos. Soc.* **87**, 128-162 (2012).
17. U. Rowlatt, N. Mrosovsky, A. English, *Neonatology* **17** 53-83 (1971).
18. R. Oelkrug, G. Heldmaier, C. W. Meyer, *J. Comp. Physiol. B* **181**, 137-145 (2011).
19. R. Oelkrug *et al.*, *Nat. Comm.* **4**, 2140 (2013). doi:10.1038/ncomms3140.
20. G. Heldmaier, *Z. vergl. Physiol.* **73**, 222-247 (1971).
21. G. Alexander, J. W. Bennett, R. T. Gemmell, *J. Physiol.* **244**, 223-234 (1975).
22. L. E. Pearson, H. E. Liwanag, M. O. Hammill, J. M. Burns, *J. Therm. Biol.* **44**, 93-102 (2014).
23. D. C. Fisher *et al.*, *Quat. Int.* **255**, 94-105 (2012).
24. F. Berg, U. Gustafson, L. Andersson, *PLoS Genet.* **2**, e129 (2006). doi:10.1371/journal.pgen.0020129.
25. Materials and methods are available as supplementary materials on *Science* Online.
26. R. W. Meredith, J. Gatesy, W. J. Murphy, O. A. Ryder, M. S. Springer, *PLoS Genet.* **5**, e1000634 (2009). doi:10.1371/journal.pgen.1000634.

27. B. K. McNab, in *The Evolution and Ecology of Armadillos, Sloths and Vermilinguas*, G. G. Montgomery, Ed. (Smithsonian Institution Press, Washington, 1985), pp. 219-232.
28. M. E. Heath, H. T. Hammel, *Am. J. Physiol.* **250**, R377-R382 (1986).
29. P. R. Morrison, *J. Mammal.* **26**, 272-275 (1945).
30. M. Superina, P. Boily, *Comp. Biochem. Physiol A*, **148**, 893-898 (2007).
31. C. W. Meyer *et al*., *Am. J. Physiol.* **299**, R1396-R1406 (2010).
32. P. F. Scholander, *Evolution* **9**, 15-26 (1955).
33. S. R. Pant, A. Goswami, J. A. Finarelli, *BMC Evol. Biol.* **14**, 184 (2014). doi:10.1186/s12862-014-0184-1.
34. H. G. McDonald, C. R. Harington, G. De Iuliis, *Arctic* **53**, 213-220 (2000).
35. C. De Muizon, H. G. McDonald, *Nature* **375**, 224-227 (1995).
36. C. M. Janis, *Annu. Rev. Ecol. Syst.* **24**, 467-500 (1993).
37. B. G. Lovegrove, M. O. Mowoe, *J. Evol. Biol.* **26**, 1317-1329 (2013).
38. E. Gheerbrant *et al*., *Proc. Nat. Acad. Sci. U.S.A.* **106**, 10717-10721 (2009).
39. E. Gheerbrant, D. P. Domning, P. Tassy, in *The Rise of Placental Mammals: Origins and Relationships of the Major Extant Clades*, K. D. Rose, J. D. Archibald, Eds. (Johns Hopkins Univ. Press, Baltimore, 2005), pp. 84-105.
40. E. Barrow, E. R. Seiffert, E. L. Simons, *J. Syst. Palaeontol.* **8**, 213-244 (2010).
41. R. D. Guthrie, *Nature* **426**, 169-171 (2003).
42. O. Hashimoto *et al.*, *PLoS ONE* **10**, e0116734 (2015). doi:10.1371/journal.pone.0116734.
43. K. N. Lewis *et al*., *Mamm. Genome* **27**, 259-278 (2016).
44. S. Bajpai, P. D. Gingerich, *Proc. Natl. Acad. Sci. U.S.A.* **95**, 15464-15468 (1998).
45. P. D. Gingerich, in *The Emergence of Whales: Evolutionary Patterns in the Origin of Cetacea.* J. G. M. Thewissen, Ed. (Plenum, New York, 1998), pp. 423-449.
46. D. P. Domning, *Hist. Biol.* **14**, 115-119 (2000).
47. M. D. Uhen, *Annu. Rev. Earth Planet. Sci.* **38**, 189-219 (2010).
48. F. Bokma *et al*., *Syst. Biol*. **65**, 98-108 (2016).
49. W. P. Maddison, P. E. Midford, S.P. Otto, *Syst. Biol.* **56**, 701-710 (2007).
50. R. G. FitzJohn, *Methods Ecol. Evol.* **3**, 1084-1092 (2012).
51. J. Nedergaard *et al.*, *Biochim. Biophys. Acta* **1504**, 82-106 (2001).
52. M. Cardillo *et al*., *Science* **309**, 1239-1241 (2005).
53. N. C. Bal *et al*., *Nat. Med.* **18**, 1575-1579 (2012).
54. L. A. Rowland, N. C. Bal, L. P. Kozak, M. Periasamy, *J. Biol. Chem.* **290**, 12282-12289 (2015). doi: 10.1074/jbc.M115.637603.

Acknowledgments:
We thank Stephen Petersen, John Gatesy, Cheryl Y. Hayashi, Ross D.E. MacPhee, Eske Willerslev, Mads Bertelsen, R. Havmøller, and Tom Gilbert for providing tissue samples, Oliver Friedrich for assistance with $\delta^{18}O$ isotope to temperature conversions, and Mark Uhen and Felisa Smith for providing access to the MAMMOTH v1.5 database. Authorization to use paintings by Carl Buell was provided by John Gatesy. M.J.G. was funded in part by a University of Manitoba Undergraduate Research Award, a University of Manitoba Graduate Fellowship, and a Manitoba Graduate Fellowship. J.L.A.P. was funded in part by a Natural Environment Research Council (NERC) student fellowship

and the University of York. A.V.S. was funded in part by a National Sciences and Engineering Research Council (NSERC) Alexander Graham Bell Canada Graduate Scholarship–Doctoral Program. This work was supported by NSERC Discovery Grants to K.L.C. (238838) and J.R.T. (418503), an NSERC Discovery Accelerator Supplement to K.L.C. (412336), the Canada Research Chairs program to J.R.T. (950-223744), a German Center for Diabetes Research (DZD) grant to M.J., and a NSF grant (EF0629860) to M.S.S.

Supplementary Materials:

Materials and Methods

Supplementary Text

Figures S1-S4

Tables S1-S7

References (55-195)

Data Files S1-S10

Figure legends

Fig. 1. Schematic illustrating disrupting mutations in *ucp1* across the placental mammal phylogeny. (**A**) Xenarthra, (**B**) Pholidota, (**C**) Cetacea; note insert from ~800 bp upstream of *ucp1* exon 4 of beluga (orange), (**D**) Suidae, (**E**) Paenungulata; *putative start codon located 36 bp downstream, **creates 15 downstream stop codons (not shown), (**F**) Equidae. The six coding exons of *ucp1* are represented by open rectangles; missing data (black), deleted exons (grey), mutated start codons (green), nonsense mutations (red), deletions (magenta), insertions (cyan), splice site mutations (yellow), and a mutated stop codon ('TTA' in *Cyclopes*) are indicated.

Fig. 2. Large scale deletions of the uncoupling protein 1 (*ucp1*) locus in select placental species. (**A**) Linear comparisons of *ucp1* illustrating exon deletions in pangolin, armadillo, pig, and hyrax relative to the intact human locus. The coding exons of *ucp1* are numbered and highlighted in red. (**B**) Patterns of conserved synteny in the

genomic region flanking the *ucp1* locus of select vertebrates illustrating the complete deletion of *ucp1* in a common ancestor of the dolphin and killer whale. Coding exons are highlighted in red, intervening sequences are highlighted in grey, while sequencing gaps are denoted by white spaces. Distances in kilobases (kb) between the termination codons of the upstream (*tbc1d9*) and downstream (*elmod2*) loci are given for each species. Note that the platypus *ucp1* locus contains an additional upstream exon relative to other vertebrate species. Artwork by Carl Buell.

Fig. 3. UCP1 inactivation across a time-calibrated placental mammal phylogeny. Functional *ucp1* branches are denoted in black, pseudogenic branches in red, and mixed branches (where *ucp1* inactivation occurred) in blue. Clades possessing intact *ucp1* loci are collapsed. Red boxes indicate *ucp1* inactivation date ranges as determined by d*N*/d*S* analyses (see table S3), while the dagger represents the complete deletion of this locus in the delphinid lineage (see Fig. 2B). Pre-Oligocene temperatures are based upon a benthic foraminifera $\delta^{18}O$ isotope dataset assuming an ice-free ocean (*25*). Note that the majority of inactivations correspond to a period of intense global cooling (grey shading) following the Paleocene-Eocene Thermal Maximum (PETM). Within this window, *ucp1* was inactivated earlier in the two aquatic species, consistent with the much higher thermal conductivity of water relative to air (~24.1× higher at 25ºC). As only remnants of *ucp1* were identified from representative Pilosa (*Bradypus*, *Choleopus*, *Cyclopes*), that moreover did not share common inactivating mutations with Cingulata, we were unable to reliably date its inactivation in this clade. Artwork by Carl Buell.

Fig. 4. Body mass and taxon diversity relative to estimates of *ucp1* inactivation in five lineages of eutherian mammals. (**A**) Calculated *ucp1* inactivation range (red shading) in relation to body size estimates (open and closed circles). The y-axis is reduced in the insets to better visualize changes in body mass relative to *ucp1* inactivation. (**B**) Calculated *ucp1* inactivation range (red shading) in relation to records of the number of species (closed squares) and genera (open squares) per geological stage. Blue arrows denote current species diversity for each taxon.

Figure 1

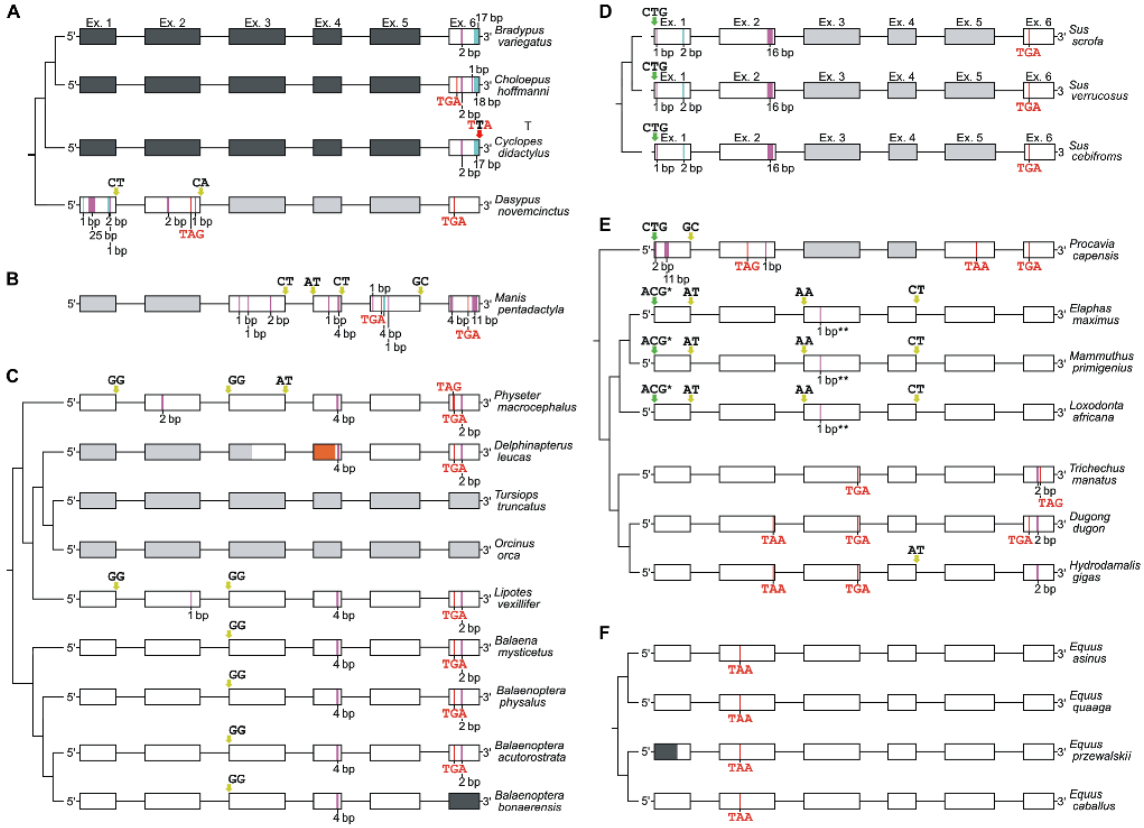

Figure 2

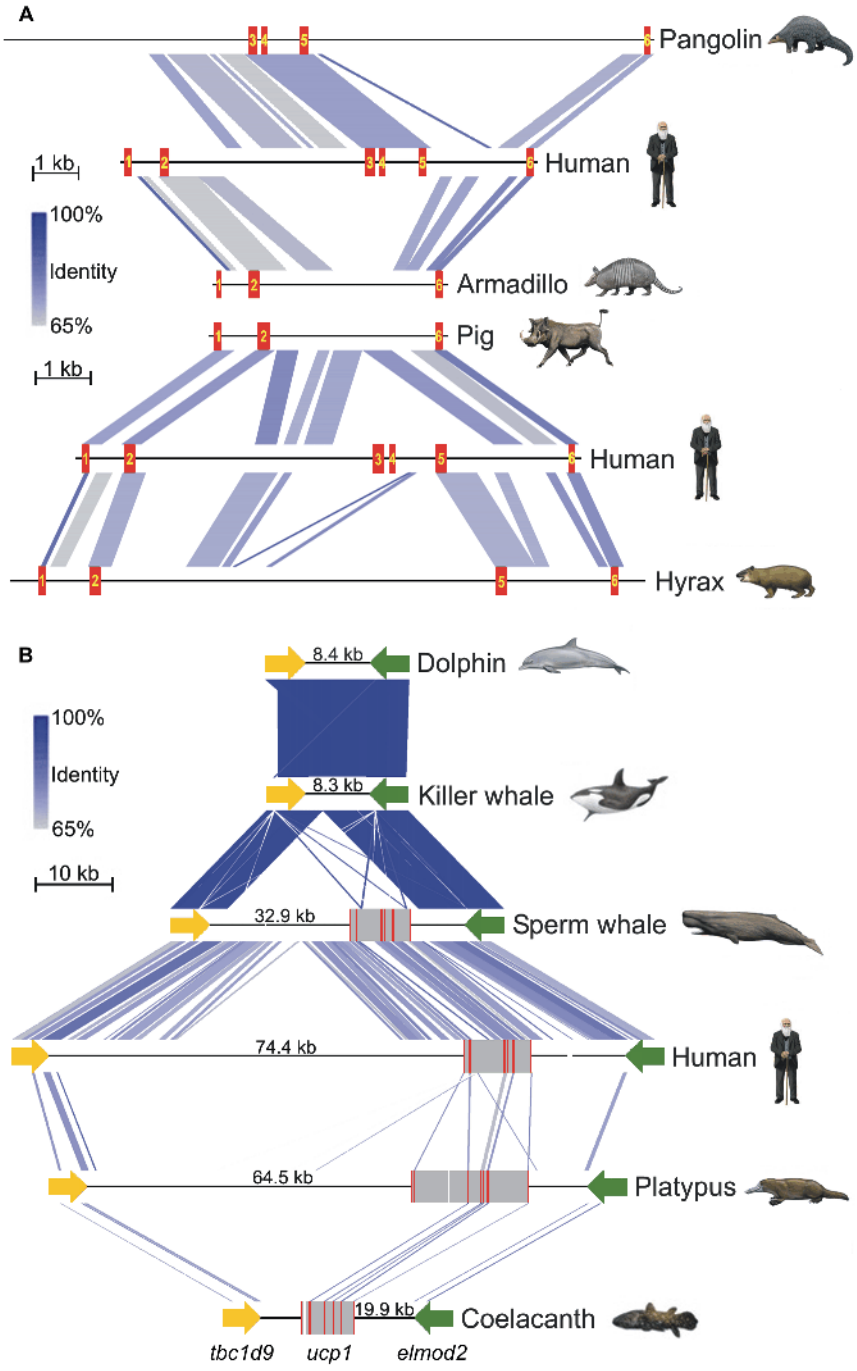

Figure 3

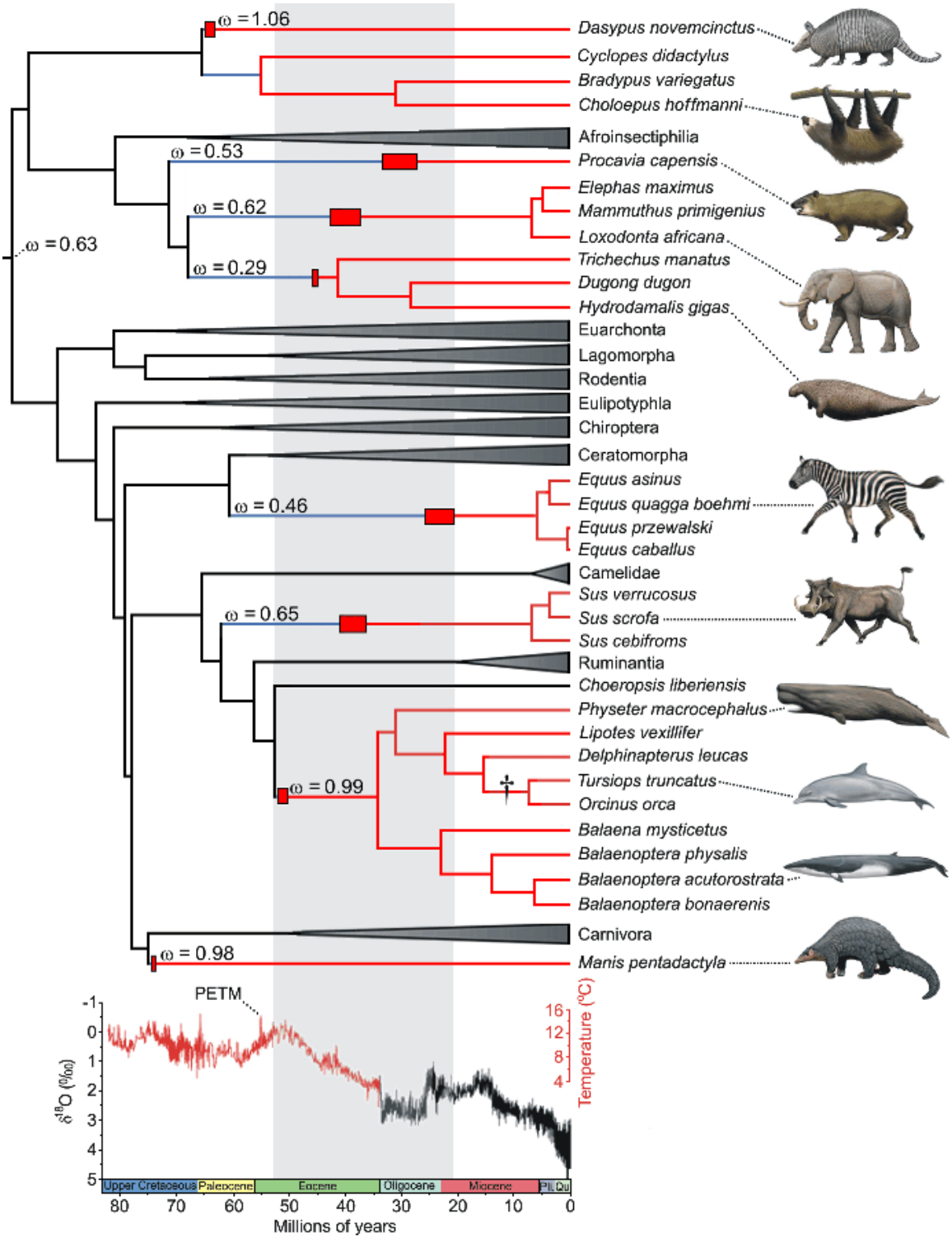

Figure 4